SUPPLEMENTARY INFORMATION

A compact integrated microfluidic oxygenator with high gas exchange efficiency and compatibility for long-lasting endothelialization.

Received 00th January 20xx,
Accepted 00th January 20xx

DOI: 10.1039/x0xx00000x

* https://orcid.org/0000-0001-7514-244X

Julie Lachaux,[a] Gilgueng Hwang,[a] Nassim Arouche,[b] Sina Naserian,[a-b] Abdelmounaim Harouri,[a] Valeria Lotito,[a] Caterina Casari,[c] Thevy Lok,[d] Jean Baptiste Menager[e], Justin Issard[e], Julien Guihaire[e], Cécile V. Denis,[c] Peter J. Lenting,[c] Abdul I. Barakat,[d] Georges Uzan,[b] Olaf Mercier,[e] and Anne-Marie Haghiri-Gosnet*[a]

[a.] *Address here.*
[b.] *Address here.*
[c.] *Address here.*

† Footnotes relating to the title and/or authors should appear here.
Electronic Supplementary Information (ESI) available: [details of any supplementary information available should be included here]. See DOI: 10.1039/x0xx00000x

SUPPLEMENTARY INFORMATION

SI.1 Theoretical calculations

SI.1A. Calculating the effective solubility and diffusivity of O_2 in blood (model of Potkay 2013 [1])

The oxygen-hemoglobin dissociation, described by the Hill equation [2], is given below:

$$SatO_2 = \frac{(PO_2 / P_{50})^n}{1 + (PO_2 / P_{50})^n}$$

Where P_{50} is the partial pressure of oxygen where the blood is 50% saturated ($SatO_2$=0,5) and *n* is the Hill coefficient. For porcine blood in normal condition (T=37°C et pH=7,4), P_{50} and *n* are estimated to be 35,7 mmHg and 2,94 [3].

The effective solubility and diffusivity of oxygen in blood in the device, $S_{B,\ O_2}$ and D_{B,O_2}, are defined as the effective solubility and diffusivity of O_2 averaged over the range of O_2 partial pressures (PO_2) in blood between the inlet and the outlet of the capillaries. The equations and settings presented below are explained in detail in the article of Potkay 2013 [1].

$$S_{B,\ O_2} = \frac{\int_{P_{O_2,min}}^{P_{O_2,max}} \alpha_{eff,O_2}\ dP_{O_2}}{P_{O_2,max} - P_{O_2,min}}$$

$$D_{B,O_2} = \frac{\int_{P_{O_2,min}}^{P_{O_2,max}} D_{eff,O_2}\ dP_{O_2}}{P_{O_2,max} - P_{O_2,min}}$$

where $P_{O_2,min}$ is the expected oxygen partial pressure at the inlet of the blood capillary, $P_{O_2,max}$ is the expected oxygen partial pressure at the outlet of the blood capillary, α_{eff,O_2} is the effective solubility of O_2 in blood at a specific PO_2, and D_{eff,O_2} is the effective diffusivity of O_2 in blood at a specific PO_2.

$$D_{eff,O_2} = \frac{D_{pl,O_2}}{1 + c_T \frac{\lambda_{O_2}(PO_2)}{\alpha_{pl,O_2}}}$$

$$\alpha_{eff,O_2} = \alpha_{pl,O_2} + c_T \times \lambda_{O_2}(PO_2)$$

where D_{pl,O_2} is the diffusivity of oxygen in blood plasma, α_{pl,O_2} is the solubility of oxygen in blood plasma, c_T = 1,39 Hct/3 is the oxygen binding capacity of hemoglobin (ml O_2/ml blood), Hct is the hematocrit, $\lambda_{O_2}(PO_2)$ is the slope of the oxygen-hemoglobin dissociation curve ($dSatO_2/dPO_2$) for a given partial oxygen pressure (PO_2).

Used settings:

- D_{pl,O_2} = 1,8x10^{-5} cm²/s
- α_{pl,O_2}= 3x10^{-5} ml O_2/ml sang/mmHg
- Hct = 33%
- c_T = 1,39 *Hct*/3 = 0,1529
- P_{50} = 35,7 mmHg
- $n = 2{,}94$
- $P_{O_2,max}$ = 195 mmHg
- $P_{O_2,min}$ = 45 mmHg

SI.1B. Calculating the effective solubility and diffusivity of CO_2 in blood (model of Potkay 2013 [1])

An equation relating the volume percentage of CO_2 in blood to the CO_2 partial pressure (PCO_2) in blood was described by Mochizuki et al. [4], as given below:

$$C_B = \frac{A_M \times {B_M}^{-2{,}548} \times {PCO_2}^{B_M}}{100}$$

where C_B is the volume percentage of CO_2 in blood, A_M and B_M are constants. A_M is estimed to be 1,07 and B_M is estimated to be 0,46 for a veinous blood.

The effective solubility and diffusivity of carbon dioxide in blood in the device, $S_{B,\ CO_2}$ and D_{B,CO_2}, are defined as the effective solubility and diffusivity of CO_2 averaged over the range of CO_2 partial pressures (PCO_2) in blood between the inlet and the outlet of the capillaries. The equations and settings presented below are explained in detail in the article of Potkay 2013 [1].

$$S_{B,\ CO_2} = \frac{\int_{P_{CO_2,min}}^{P_{CO_2,max}} \alpha_{eff,CO_2}\ dP_{CO_2}}{P_{CO_2,max} - P_{CO_2,min}}$$

$$D_{B,CO_2} = \frac{\int_{P_{CO_2,min}}^{P_{CO_2,max}} D_{eff,CO_2}\ dP_{CO_2}}{P_{CO_2,max} - P_{CO_2,min}}$$

where $P_{CO_2,min}$ is the expected carbon dioxide partial pressure at the inlet of the blood capillary, $P_{CO_2,max}$ is the expected carbon dioxide partial pressure at the outlet of the blood capillary, α_{eff,CO_2} is the effective solubility of CO_2 in blood at a specific PCO_2, and D_{eff,CO_2} is the effective diffusivity of CO_2 in blood at a specific PCO_2.

$$D_{eff,CO_2} = \frac{D_{pl,CO_2}}{\frac{\lambda_{CO_2}(PCO_2)}{\alpha_{pl,CO_2}}}$$

$$\alpha_{eff,CO_2} = \lambda_{CO_2}(PCO_2)$$

Where $D_{pl,CO_2}$is the diffusivity of carbon dioxide in blood plasma, α_{pl,CO_2} is the solubility of oxygen in blood plasma, $\lambda_{CO_2}(PCO_2)$ is the slope of the CO_2 volume percentage curve ($dC_B/dPCO_2$) for a given CO_2 partial pressure.

Used settings:

- $A_M = 1{,}07$
- B_M = 0,46
- α_{pl,CO_2}= 6x10^{-4} ml CO_2 /ml sang/mmHg
- D_{pl,CO_2}= 2,5x10^{-5} cm²/s
- $P_{CO_2,max}$ = 60 mmHg
- $P_{CO_2,min}$ = 20 mmHg

SI.1C. Calculating the O_2 uptake and CO_2 release

The O_2 uptake for different flow rates was calculated by summing the amount of dissolved oxygen in blood and the amount of oxygen molecules bound to hemoglobin, based on the equation [5,6]:

$$\frac{\Delta ctO_2}{\Delta t} = Q\left[S_{O_2,\,plasma} \times \Delta PO_2 + 1{,}39 \times ctHb(g) \times \Delta SatO_2\right]$$

where $\frac{\Delta ctO_2}{\Delta t}$ is the O_2 uptake (ml O_2/min); $S_{O_2,\,plasma}$ is the solubility coefficient of O_2 in plasma (3.14 10^{-5} ml O_2/mmHg/ml blood) ; ΔPO_2 is the oxygen partial pressure variation between the inlet and the outlet of the device (mmHg) ; 1,39 ml O_2/ g Hb is theoretical O_2 binding capacity of haemoglobin ; $ctHb(g)$ is the concentration of haemoglobin in blood (g Hb/ ml blood): for swine, $ctHb(g)$ is estimated to be 0,10 g/ml [8,9]; $\Delta SatO_2$ is the oxygen saturation variation between the inlet and the outlet of the device (unitless).

The CO_2 release for different flow rates was calculated by summing the amount of carbon dioxide in plasma (dissolved and in the form of bicarbonate) and in erythrocytic fluid, based on the equation [6,7]:

$$\frac{\Delta ctCO_2(S)}{\Delta t} = Q\left[9{,}286 \times 10^{-3} \times \Delta PCO_2 \times ctHb \times \left(1 + 10^{pH_{ery} - pK_{ery}}\right) + ctCO_2(P)\left(1 - \frac{ctHb}{21}\right)\right]$$

$$pH_{ery} = 7{,}19 + 0{,}77\,(pH - 7{,}40) + 0{,}035\,(1 - SatO_2)$$

$$pK_{ery} = 6{,}125 - \log\left(1 + 10^{pH_{ery} - 7{,}84 - 0{,}06 \cdot SatO_2}\right)$$

$$ctCO_2(P) = S_{CO_2,\,plasma} \times \Delta PCO_2 + cHCO_3(P)$$

$$cHCO_3(P) = S_{CO_2,\,plasma} \times \Delta PCO_2 \times 10^{pH\,-\,pK(P)}$$

$$pK(P) = 6{,}125 - \log\left(1 + 10^{pH\,-\,8{,}7}\right)$$

where $\frac{\Delta ctCO_2(S)}{\Delta t}$ is the CO_2 release (ml CO_2/min) ; ΔPCO_2 is the carbon dioxide partial pressure variation between the inlet and the outlet of the device (kPa) ; $ctHb$ is the concentration of haemoglobin in blood (mmol Hb/L sang): for swine, $ctHb(g)$ is estimated to be 0,10 g/ml which is equivalent to 6,21 mmol/L ; pH_{ery} is the pH of erythrocyte (unitless) ; $SatO_2$ is the oxygen saturation (unitless) ; pK_{ery} is a constant related to erythrocyte (unitless) ; $ctCO_2(P)$ is the concentration of CO_2 in plasma (mmol CO2/ L blood) ; $S_{CO_2,\,plasma}$ is the solubility of carbon dioxide in blood plasma at the considered temperature : 0,230 mmol/L/kPa ; $cHCO_3(P)$ is the concentration of bicarbonate in plasma (mmol HCO_3^- / L blood) ; $pK(P)$ is a constant related to blood plasma (unitless).

SI.2. In vitro experiments: comparison of pure oxygen and air

In order to identify the influence of the oxygen concentration in the gas on both oxygenation and decarbonatation, two devices with different oxygenation gas have been analyzed. In the first device, pure oxygen was used while in the second device a mixture of air/oxygen (50/50) was injected into the gas network. The height of the blood capillaries and the oxygenation micro-channels was fixed at 85 µm. The variation of oxygen and carbon dioxide partial pressures between the inlet and outlet of the device (ΔPO_2 and ΔPCO_2) and the oxygen saturation at the outlet of the device ($SatO_2$) were analyzed for a blood flow rate ranging from 0.5 to 15 ml/min. Results are shown in figure SI.2.

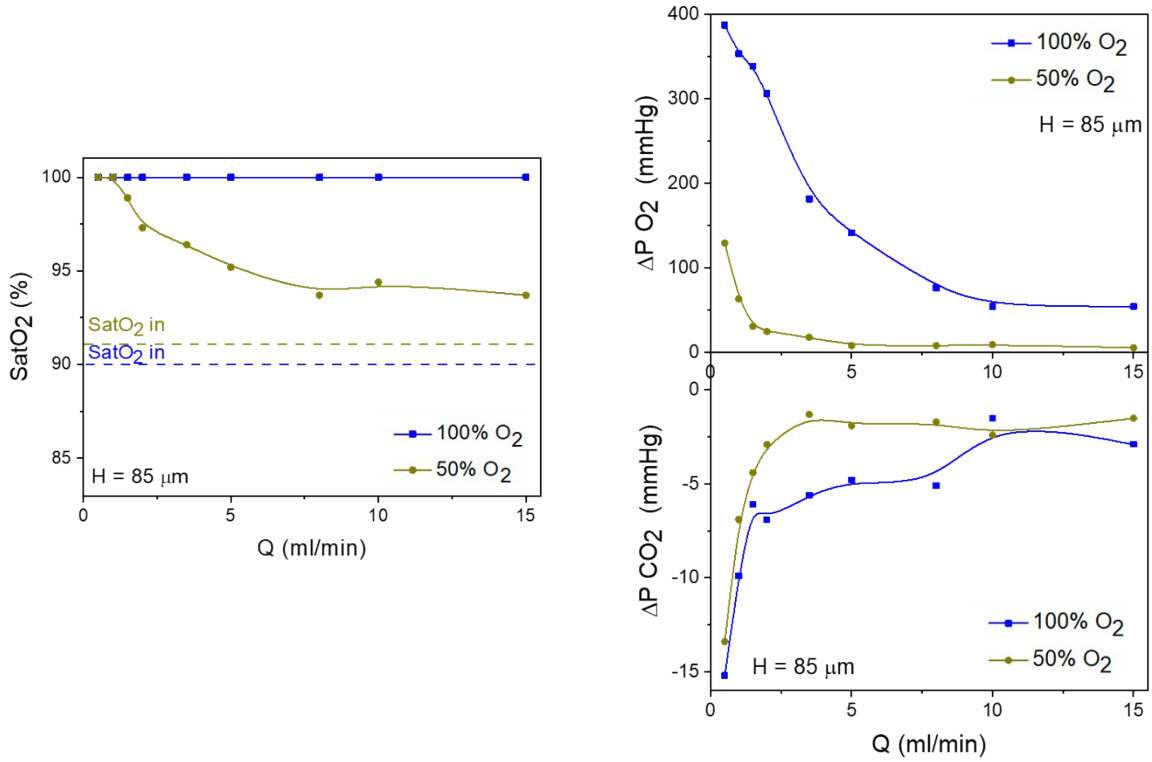

Fig SI.2. *In vitro* performance of single-layer devices (with H = 85 µm) compared for the two gases studied: air or pure oxygen: (a) variation of the oxygen saturation level $SatO_2$ measured in the blood collected at the output (dotted lines give the input values), (c) variation of the oxygen partial pressure ΔPO_2 and (b) carbon dioxide partial pressure ΔCO_2.

ΔPO_2 is much smaller with the mixture of air/oxygen than with pure oxygen for all blood flow rates. At the maximum blood flow rate of 15 ml/min, ΔPO_2 is about 5.6 mmHg with the mixture of air/oxygen, while it reaches 54.5 mmHg with pure oxygen. ΔPCO_2 takes the same value for both gas oxygenation at very low flow rates (from 0.5 ml/min to 1.5 ml/min) and high flow rates (from 10 and 15 ml/min). However, in the range of 2 - 8 ml/min, one can observe different ΔPCO_2 values. This is surprising since the percentage of oxygen in the oxygenation gas should not change the carbon dioxide partial pressure. Indeed, the concentration of carbon dioxide is negligible (0.04%) in air. It would be interesting to repeat this experiment on several devices to quantify measurement errors.

As expected, the oxygen saturation at the outlet is lower with the mixture of air/oxygen than with pure oxygen at flow rates higher than 1.5 ml/min. Above 5 ml/min, $SatO_2$ with the mixture of air/oxygen is less than 95% despite a very high inlet value of 91%. For comparison, $SatO_2$with pure oxygen is 100% for all blood flow rates up to 15 mL/min.

We can conclude that the oxygen percentage of the gas oxygenation is one of the most important parameters for oxygenation capacity. For this reason, we decided to work with pure oxygen in order to increase the rate of oxygen transfer to the extent possible.

SI.3 – Predictive theoretical calculations

In order to identify the influence of membrane thickness and exchange surface area on O_2 uptake and CO_2 release as function of blood flow rate, theoretical calculations of O_2 uptake and CO_2 release (see part.2.1 in the article and SI.1 in supplementary information) have been done based on the mathematical model of Potkay [4].

SI.3A. Simulations: role of the membrane thickness (15µm < e_m < 105µm)

Theoretical O_2 uptake and CO_2 release are presented below as a function of blood flow rate Q (1; 5; 10; and 15 ml/min) for different membrane thickness e_m (15, 45, 75 and 105 µm). As expected, the higher the blood flow rate and the thinner the membrane thickness, the better are the O_2 uptake and the CO_2 release.

As observed in the resistance equation [4] (see part.2.1 in the main text with $R_{O_{2,tot}} = \frac{e_m}{P_{m,O_2}} + \frac{\frac{H}{2}}{S_{B,O_2} \cdot D_{B,O_2}}$), lowering the membrane thickness allows reducing the resistance to diffusion. Concerning O_2 uptake, we observe that the effect of the membrane thickness is noticeable only at high blood flow rate in the range from 10 to 15 ml/min. Whereas at low flow rate (Q<5ml/min), blood has enough time to be almost fully oxygenated (Sat(O_2)~ 100%) even for the thickest membrane of 105 µm, at high blood flow rate (Q>10ml/min), the retention time is sufficiently reduced to make the effect of thin membrane thickness observable. Concerning CO_2 release, the effect of membrane thickness is more pronounced at every blood flow rate. Reducing the thickness of the membrane is therefore important for the O_2 uptake only at high blood flow rate and for the CO_2 release regardless every blood flow rate.

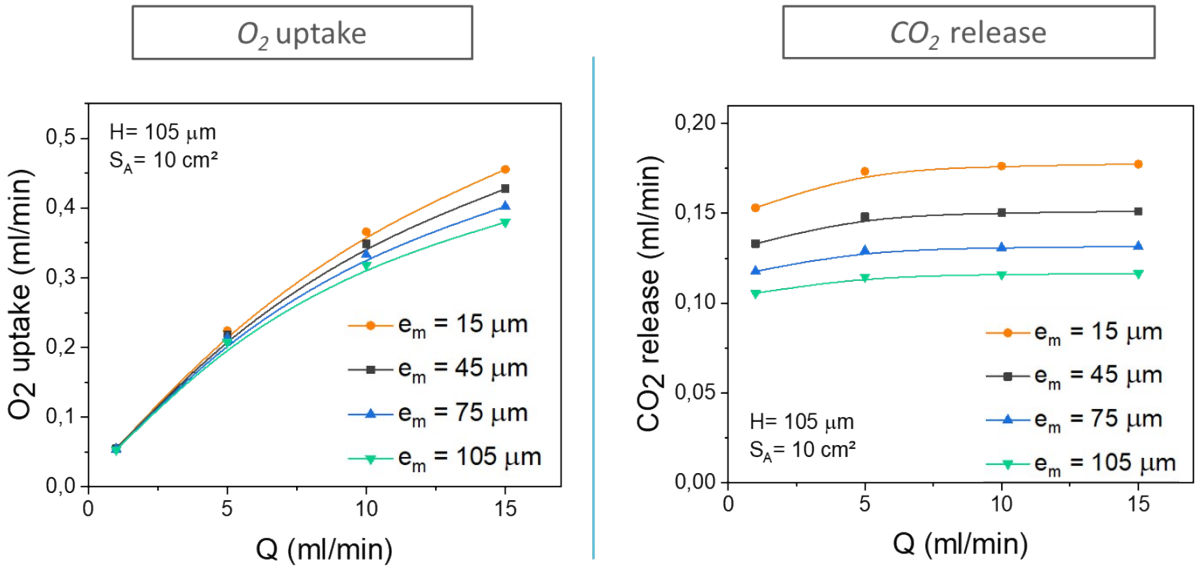

SI.3B. Simulations: role of the exchange surface area (10 cm² < S_A < 40 cm²)

Theoretical O_2 uptake and CO_2 release are presented below as a function of blood flow rate for different exchange surface area S_A (10, 20, 30 and 40 cm²). As expected, the higher the blood flow rate and the larger the exchange surface area, the better are the O_2 uptake and the CO_2 release. Concerning O_2 uptake, similarly as the previous simulation, the effect of exchange surface area is more pronounced at high blood flow rate and particularly between 10 and 20 cm². Concerning CO_2 release, the effect of the exchange surface area is

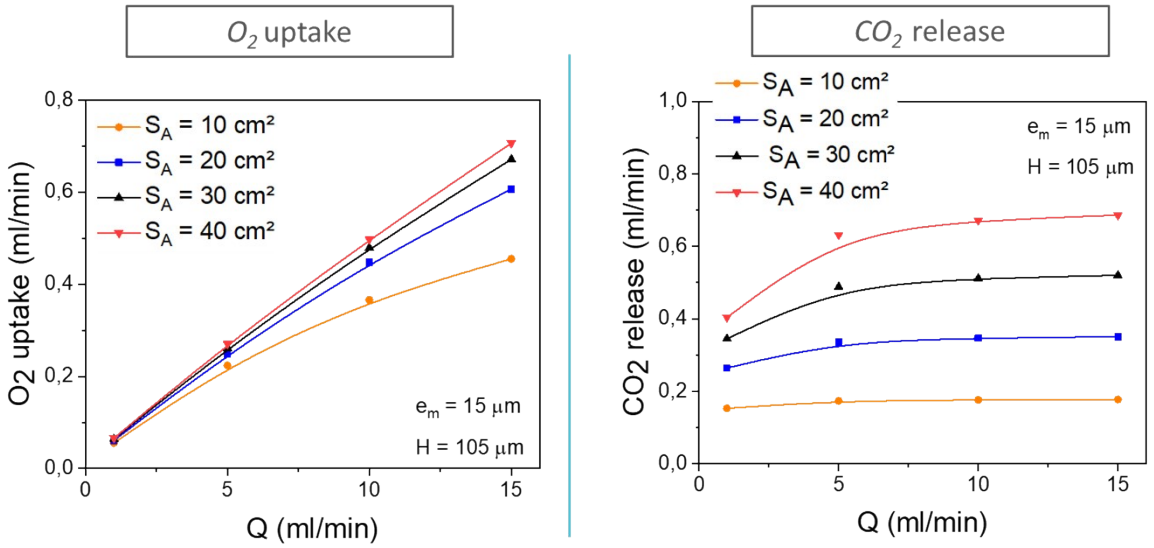

significant at every blood flow rate.

To conclude, from these simulations (SI.3A and SI.3B), the exchange surface area has a larger impact on gas transfer efficiency than the membrane thickness, especially for the CO_2 release. Therefore, it appears very important to enhance as much as possible the exchange surface area. This can be done easily without altering the other properties (such as pressure drop) by realizing a device with a double-sided diffusion, with two integrated membranes at the bottom and the top of the blood capillaries similarly as in the work of Rieper [10]. The device can also be expanded laterally but in this case the capillaries will be longer, so the pressure drop in the whole system should be reconsidered.

SI.4. In vitro experiments: pictures and videos recorded for stacked devices during blood filling

For videos:

3-stacked unit device: file “video1.mpeg” and 5-stacked unit device: file “video2.mpeg”

3-units stacked device (25ml/min)

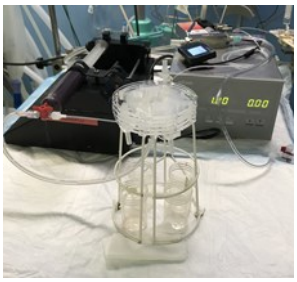

5-units stacked device (80

SI.5. In vitro experiments: ΔPO_2 and ΔPCO_2 between the outlet and the inlet of the device for 3 and 5 stacked units layers

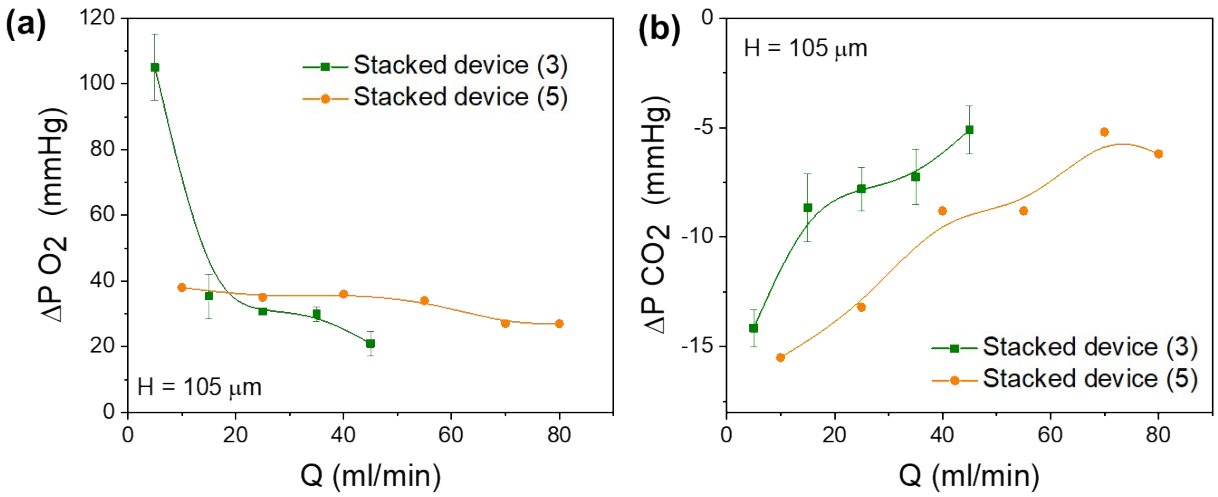

SI.6. In vitro experiments: comparison of experimental O_2 uptake and CO_2 release per unit layer as a function of blood flow rate for one single unit layer, 3- and 5- stacked unit devices

O_2 uptake and CO_2 release per unit layer as a function of blood flow rate per unit layer is shown here. These graphs allow to compare the oxygenation and decarbonation efficiency per unit layer for one single or more units stacked in parallel.

Concerning the first graph, O_2 uptake per unit layer is a bit enhanced for 3- and 5- stacked units at high blood flow rate in the range 10 to 15 ml/min. For the second graph, CO_2 release per unit layer is also enhanced for 3- and 5- stacked unit devices in the range 5 to 15 ml/min.

Concerning CO_2 release, one main factor is involved: carbon dioxide partial pressure at the inlet of the device ($PCO_{2,in}$) was too low at the beginning of the first experiment (single unit with $PCO_{2,in}$ = 54 mmHg) compared to the second experiment (stacked units with $PCO_{2,in}$ = 63,2 mmHg). With higher $PCO_{2,in}$ the second experiment allows a better determination of the maximum CO_2 transfer capability of the device.

Moreover, O_2 uptake and CO_2 release increase slightly with the number of stacked layers. This enhancement can be explained by the proximity of the adjacent parallel blood channels that can be oxygenated by the sandwiched gas channels. The results on CO_2 release is more significant as the CO_2 release is more dependent on the exchange surface area (see SI.3.B).

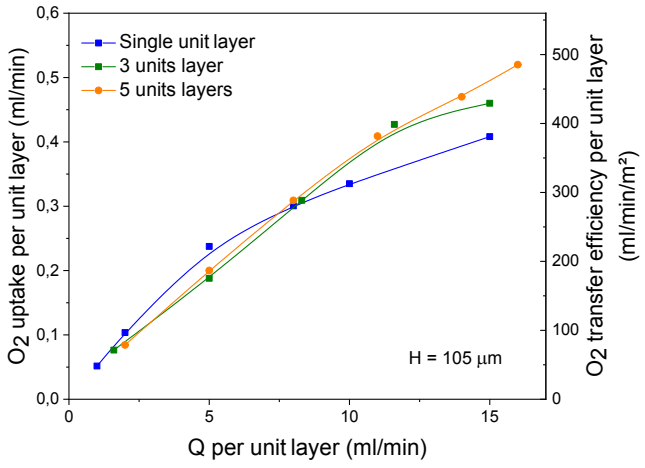

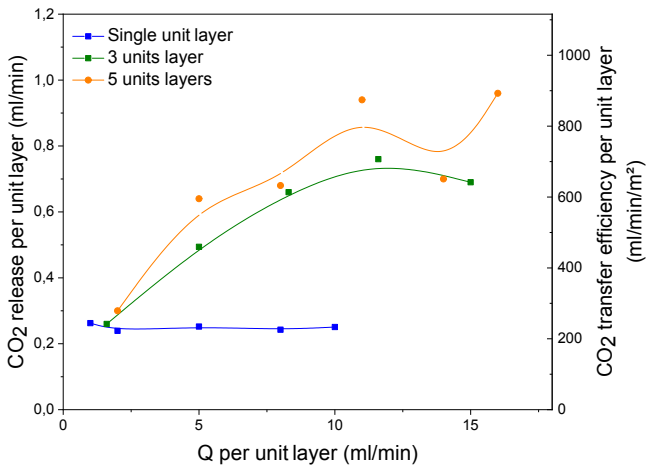

These results confirm that realizing a double-membrane stacked device could be a good way to further increase O_2 and CO_2 efficiency per unit layer as the exchange surface area will be twice as large.

References

1. J. A. Potkay, *Biomedical Microdevices*, 2013, **15(3)**, 397–406
2. J. Barcroft, A. V. Hill, *The Journal of Physiology*, 1910, **39(6)**, 411–428
3. D. C. Willford, E. P. Hill, *Respiration Physiology*, 1986, **64(2)**, 113–123
4. M. Mochizuki, H. Takiwaki, T. Kagawa, H. Tazawa, *Japanese Journal of Physiology*, 1983, **33**, 579-599
5. P. Baele, P. Van Der Linden, *traité d'anesthésie général à mises à jour périodique, Arnette Blackwell*, 2001.
6. W.-I. Wu, N. Rochow, E. Chan, G. Fusch, A. Manan, D. Nagpal, … C. Fusch, *Lab on a Chip*, 2013, **13(13)**, 2641.
7. O. Siggaard-Andersen, P. D. Wimberley, N. Fogh-Andersen, & I. H. Gøthgen, *Scandinavian Journal of Clinical and Laboratory Investigation*, 1988, 48(sup189), 7–15.
8. R. Serianni, J. Barash, T. Bentley, P. Sharma, J. L. Fontana, D. Via, … P. D. Mongan, *Journal of Applied Physiology*, 2003, **94(2)**, 561–566.
9. C. Drieu. (2009). Thèse de doctorat. Faculté de medecine de Créteil.
10. D. T. Rieper, C. Müller and H. Reinecke, *Biomed Microdevices*, 2015, 17, 86